J Vet Diagn Invest 5:284-288 (1993)

Cariine medullary thyroid carcinoma with unusual distant metastases

Alon Harmelin, Abraham Nyska, Itamar Aroch, Boris Yakobson,
Sidi Stem, Uri Orgad, Trevor Waner

Thyroid tumors represent approximately 1-2% of all canine neoplasms[8] Of the thyroid tumors, the parafollicular cell tumors (medullary thyroid carcinoma; C-cell tumor) are rare and account for less than 5% of all canine thyroid neoplasms.[6] Medullary thyroid carcinoma metastases in dogs have been limited to the regional lymph nodes,[11] with the exception of one communication in which distant metastases have been reported.[9]

This case report describes distant uncommon metastases of a medullary thyroid carcinoma to the regional lymph nodes, liver, spleen, and prostate. Only 1 other previous report has described unusual metastases of a medullary thyroid carcinoma, without metastases to the lungs.[9] Metastases to the spleen and prostate in a dog have not been reported previously.

A lo-year-old large mixed breed dog was referred to the Koret Hebrew University with a history of chronic partial anorexia, body weight loss, and listlessness. Physical examination revealed mild depression, dull thin hair coat, pale mucous membranes, severe cachexia, muscle atrophy, and hepatomegaly. A round mass (4 x 2.5 cm) was palpated in the area on the left lateral side of the larynx, The increased size of the liver was confirmed by abdominal X-ray; in addition there was a loss of contrast between abdominal organs.

Blood was collected for complete hematology and clinical chemistry examination. HematologicaI examination revealed a normocytic normochromic anemia (PCV = 28%). The clinical pathological results were normal.

The mass was diagnosed as a thyroid tumor. A needle biopsy of the growth failed to give a more definitive diagnosis, and it was decided to investigate the hepatomegaly by exploratory laparotomy. The peritoneal cavity contained approximately 1 liter of a serosanguinous fluid and a markedly enlarged liver. On the surface of the liver there were multiple pale areas of varying size. A few of the areas- had necrotic centers. At the owner's request, the dog was euthanized.

At necropsy, the left thyroid was increased in size, encapsulated and lobulated, and on cut surface was gray-white to white (Fig. 1). The cervical lymph nodes were enlarged and firm. The liver was enlarged and diffusely infiltrated with small, white, firm centrally necrotic nodules 1-4 mm in diameter. A few white pinpoint foci were seen on the surface of the spleen. The prostate was slightly enlarged and also contained a few pinpoint focal nodules. Pulmonary edema was apparent.

Representative samples of all organs were fixed in 10% neutral buffered formalin; embedded in paraffin at 4-5 μm thickness; stained with hematoxylin and eosin (HE) and Con-

From the School of Veterinary Medicine, Hebrew University, Jerusalem, 91904 Israel (Harmelin, Aroch), Department of Pathology, Kimron Veterinary Institute, Beit Dagan Israel (Nyska, Yakobson, Orgad), Life Science Research, P.O. Box 139, Ness Ziona, 70451 Israel (Waner), and Belinson Hospital, Petach-Tiqua Israel (Stern).

Received for publication July 20, 1992.

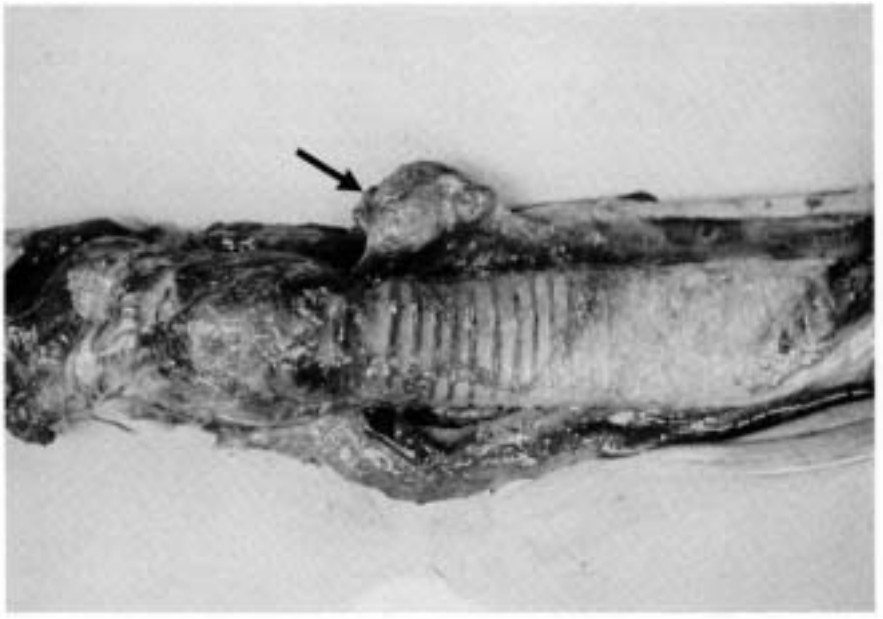

Figure 1. Medullary thyroid carcinoma in the left thyroid. Note the pale multilobulated mass (arrow).

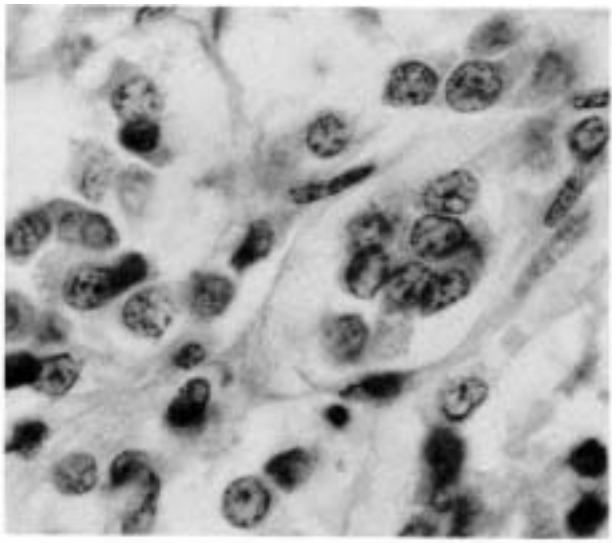

Figure 2. Photomicrograph of medullary thyroid carcinoma from the thyroid. Note the large vesiculated nuclei, prominent nucleoli, granular cytoplasm, and fibrovascular septa. HE.

go red; and examined under a light microscope. Immunohistochemical staining was performed on sections of thyroid, cervical lymph nodes, spleen, liver, and prostate using the technique described by Patnaik and Lieberman. [10] The slides were stained by the avidin-biotin-peroxidase method at the following dilutions: calcitonin (1:200),[a] neuron-specific enolase (1:100),[a] keratin (1:200),[a] and chromogranins (1:10).[a] Normal rabbit serum was used as a negative control.

The histologic pattern in the thyroid, cervical lymph nodes, liver, spleen, and prostate was similar. The tumor patterns consisted of solid sheets or nests of cells separated by fibrovascular stroma. The cells were oval to polygonal in shape, the cytoplasm was large and eosinophilic, and the nuclei were vesiculated with small nucleoli. Only a few mitotic figures were evident (Fig. 2).

The stroma within the thyroid was confirmed positive for amyloid by staining with Congo red. The hepatic cytoarchitecture was distorted by the metastatic foci of neoplastic cells along with congestion and hemorrhage in the periportal areas. The splenic cytoarchitecture was also displaced by neoplastic cells (Fig. 3). The congested lymph nodes were characterized by severe lymphoid depletion and multifocal to diffuse metastatic sites of neoplastic cells. The neoplastic cells in the prostate were distributed in nests (Fig. 4).

Immunohistochemical staining of the thyroid was positive for calcitonin; the reaction was diffuse and intracytoplasmic (Fig. 5). Focal areas of the stroma were also reactive for calcitonin. Neoplastic cells were positive for keratin; there was a heterogeneity in staining intensity among cells. Medullary thyroid carcinoma cells were also positive for neuron-specific enolase and chromogranins, the latter staining for both the nucleus and cytoplasm. Both the primary and metastatic sites showed a similar pattern of staining (Figs. 6, 7).

The tumor in the thyroid region was diagnosed as a medullary thyroid carcinoma (C-cell tumor) on the basis of histological and immunohistochemical characteristics. The serum samples were assayed for calcitonin in order to further confirm the diagnosis. Medullary carcinomas are widely known to hypersecrete calcitonin.[9,12] In this case the serum calcitonin was greatly increased (422 pg/dl) compared to the control value of 18 pg/dl. Calcium and phosphorus serum values were in the normal range, which is usually the case in dogs and humans with medullary thyroid carcinoma. Of the few clinical reports of canine medullary carcinoma only 1 dog has shown profound hypocalcemia with resultant seizures and tetany.[11]

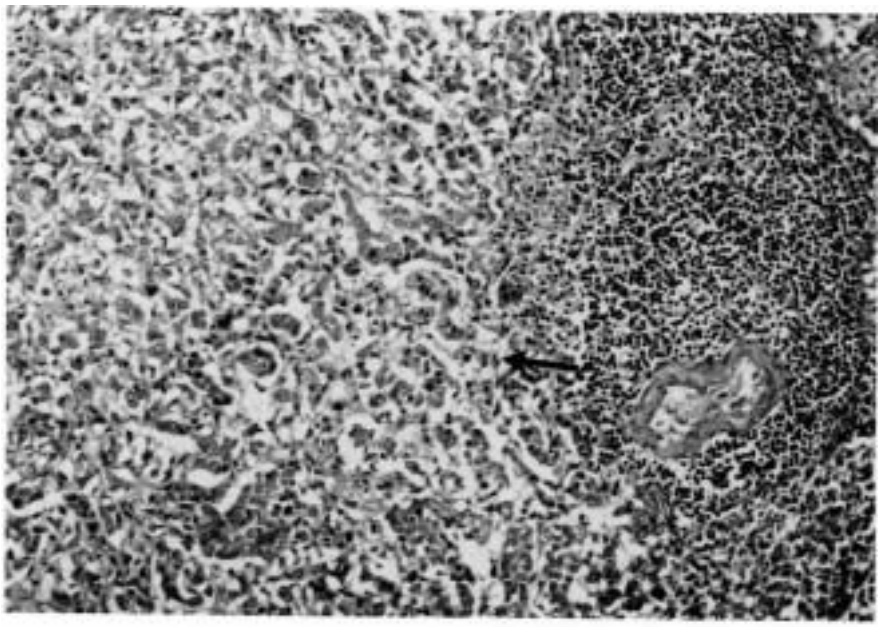

Figure 3. Photomicrograph of medullary thyroid carcinoma from the spleen. Note the neoplastic nodule growing adjacent to a lymphatic nodule (arrow). HE.

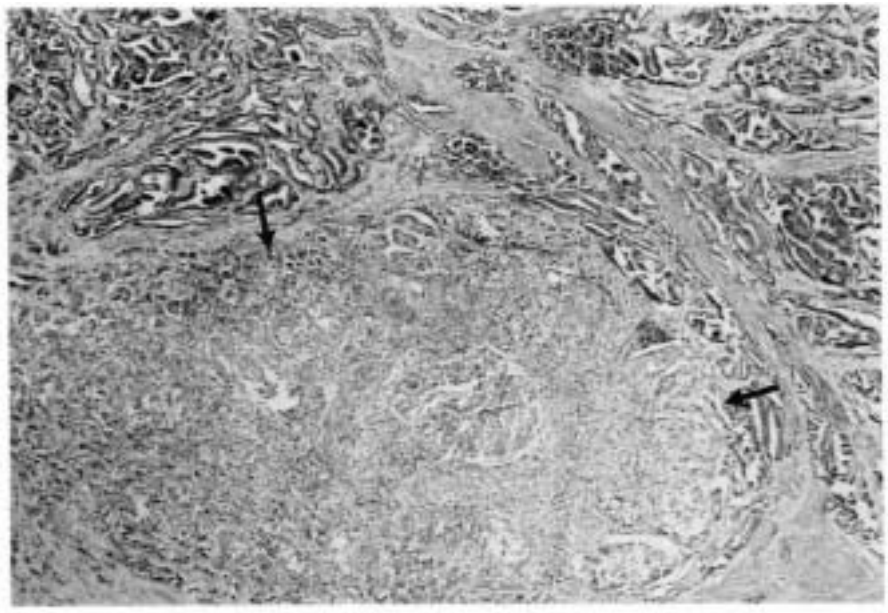

Figure 4. Photomicrograph of medullary thyroid carcinoma from the prostate. Note the multiple tumor nests surrounded by thick fibrous capsule (arrows). HE.

The light microscopic features of medullary thyroid carcinomas are distinguishable from other thyroid adenocarcinomas. The characteristic traits described in the literature are sheets of medium-sized cells separated by fibrous stroma. [12] The presence of amyloid is a variable finding in human medullary thyroid carcinomas and has been observed in 63% of canine cases.[10]

In relation to the immunohistochemical diagnostic techniques, previous studies have demonstrated that calcitonin, neuron-specific enolase, and keratin are good markers for canine medullary thyroid carcinomas.[10] Like neuron-specific enolase, chromogranins have also been shown to be a reliable marker of neuroendocrine tissue differentiation.'

The absence of tumor metastases to the lung from a neoplasm in the neck region is unusual. There is no definite reason for this phenomenon; however, this is the second case in dogs in which a medullary thyroid carcinoma has not metastased to the 1ungs.[9] It can be speculated that the pul-

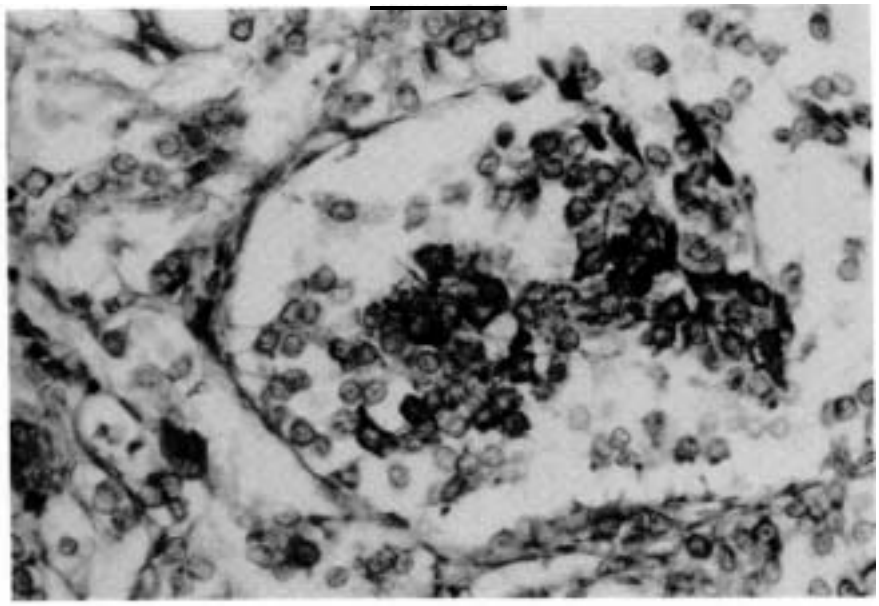

Figure 5. Photomicrograph of a medullary thyroid carcinoma from the thyroid stained against calcitonin antibody. Note the heterogeneity of staining among cells. Some of the cells have intensely staining intracytoplasmic granules. Avidin-biotin-peroxidase complex method.

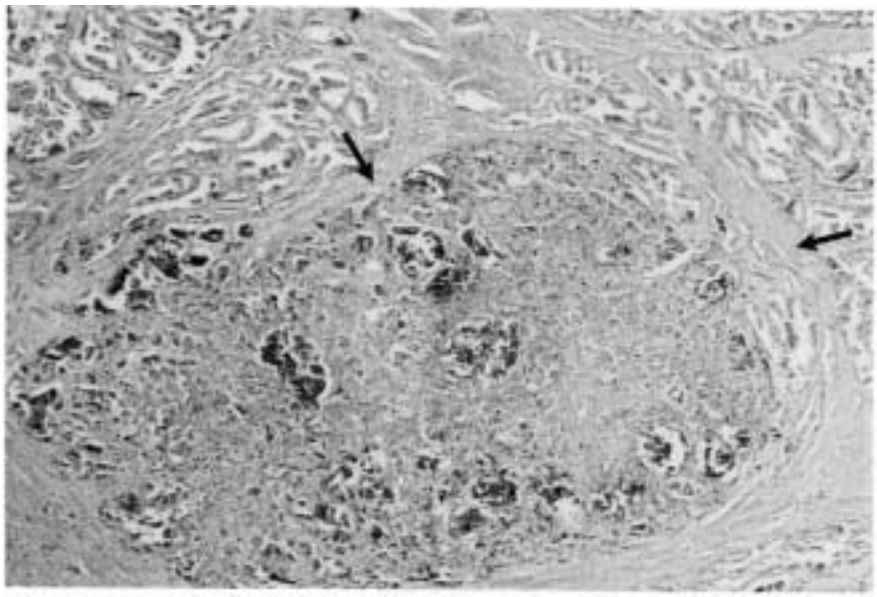

Figure 6. Photomicrograph of a medullary thyroid carcinoma from the prostate stained against neuron-specific enolase antibody. Note the positive reaction within the metastatic site (arrows). Avidin-biotin-peroxidase complex method.

monaty microenvironment was not ideal for the growth of the tumor cells[3] Furthermore, the tumor metastasized to organs in which this type of neoplasm is not usually found.

The process of cancer metastasis is complex and driven by a multitude of interactions between the disseminating tumor cells and the host tissue. Although reasons for cancer cells arresting at certain sites and not at others are not known, it is clear that some type of selectivity must occur during the development of secondary neoplasms. The predominant "seed and soil" theory suggests that tumor cells metastasize in sites that are chemically and/or physically attractive to them.[4] Experimentally, certain clones of melanomas have been shown to metastasize to specific organs.[5] The differences in the metastatic capabilities of lymphoma variants of the same tumor have also been described in the literature.[7] Differences in metastatic patterns in 2 carcinoma sublines have been attributed to variations in basement membrane-degrading enzymes, which are considered to play a key role in the process of cancer dissemination.[2]

To the best of our knowledge metastases to the prostate

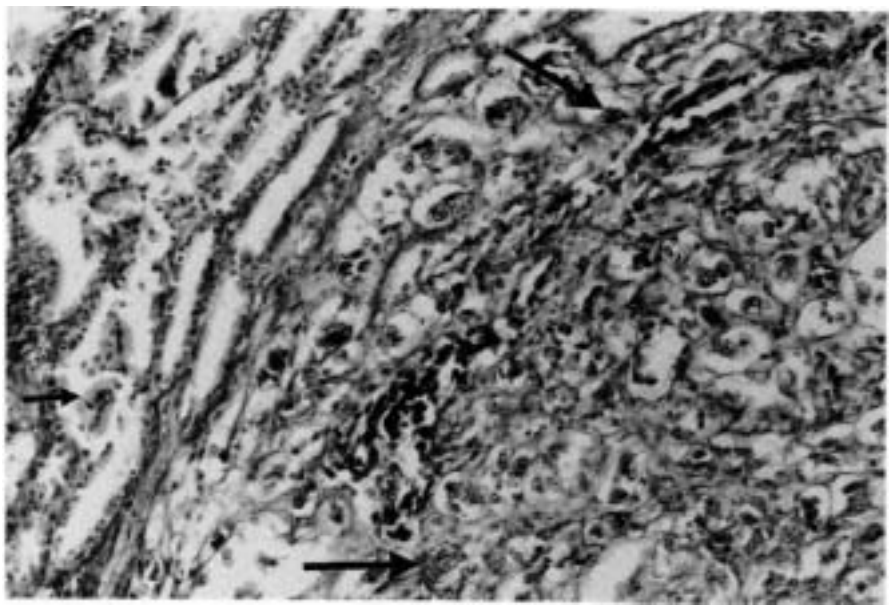

Figure 7. Photomicrograph of a medullary thyroid carcinoma from the prostate stained against calcitonin antibody. Note the positive reaction of the metastatic cells (long arrow) and the lack of reaction to the normal prostatic acinar cells (short arrow). Avidin-biotin-peroxidase complex method.

and spleen have not been previously documented in humans or dogs. This metastatic pattern may be added evidence to the distinct environmental requirements of the tumor in this case.

Sources and manufacturers

a. Dako Corp., Carpinteria, CA.

References

1. Battiflora H: 1989, Immunohistochemistry in tumor diagnosis. Handout Short Course US Can Acad Pathol, p. 33.
2. Brodt P, Reich R, Moroz LA, Chambers AF: 1992, Differences in the repertoire of basement membranes degrading enzymes in two carcinoma sublines with distinct patterns of site-selective metastasis. Biochim Biophys Acta 1139:77-83.
3. Cheville NF: 1983, Neoplasia. In: Cell pathology, 2nd ed., pp. 366-373. Iowa State University Press, Ames, IA.
4. Fidler IJ, Gersten DM, Riggs CW: 1977, Relationship of host immune status to tumor cell arrest, distribution, and survival in experimental metastatis. Cancer 40:46-55.
5. Hart IR, Fidler I J: 1980, Role of organ selectivity in the determination of metastatic patterns of B16 melanoma. Cancer Res 7:2281-2287.
6. Leav I, Schiller AL, Rijnber KA, Lagg MA, Der Kinderen PJ: 1976, Adenomas and carcinomas of the canine and feline thyroid. Am J Path01 83:61-93.
7. Leibovici J, Klein O, Argamen H, Klorin G, Michowitz: 1992, Differential metastatic capacity of three AKR lymphoma variants. Int J Exp Pathol 73:273-286.
8. Loar AS: 1986, Canine thyroid tumors. *In:* Current veterianry therapy IX, ed. Kirk RW, p. 1033. W. B. Saunders Co., Philadelphia, PA.
9. Long GG, Clemmons RM, Heath H III: 1980, Metastatic canine medullary carcinoma, a case report. Vet Path01 17:323-330.
10. Patnaik AK, Lieberman PH: 1991, Gross, histologic, cytochemical and immunocytochemical study of medullary carcinoma in sixteen dogs. Vet Pathol 28:223-233.
11. Patnaik AK, Lieberman PH, Erlandson RA, Acevedo WM, Lui S-K: 1978, Canine medullary carcinoma of the thyroid. Vet Pathol 15:590-599.
12. Peterson ME, Randolph JF, Zaki FA, Heath H III: 1982, Multiple endocrine neoplasia in a dog. J Am Vet Med Assoc 180: ***1476-1478.***

J Vet Diagn Invest 5288-290 (1993)

Aortic-iliac thromboembolism as an uncommon sequel to *Staphylococcus aureus* valvular endocarditis in a calf

Daniel G. Rudmann, Gregory W. Stevenson

Aortic-iliac thromboembolism or thrombosis has been reported in several species.[2,8,9] Affected animals usually present with a history of acute rear limb weakness or paralysis. The most common pathogenesis is the detachment of an intracardiac thrombus with subsequent lodgment at the aortic-iliac bifurcation. The condition is well documented in the cat where cardiomyopathy predisposes to intracardiac thrombus formation.[2] In dogs and birds, thrombus formation has been reported infrequently as a sequel to bacterial valvular endocarditis.[8,13]

Aortic thrombosis occurs sporadically in the horse, but the precise pathogenesis and origin of the occluding thrombus is less clear.[6] In some cases, initiation of thrombus formation is thought to occur at the aortic-iliac bifurcation. Suggested predisposing conditions include systemic infection (e.g., strangles or influenza), *Strongylus vulgaris* larval migration, back trauma, or racing-associated blood flow turbulence.[6] One case of aortic-iliac thrombosis has been reported in a calf that also had a severe necrotizing colitis. No predisposing cardiovascular lesions were noted in this calf and the authors proposed several mechanisms whereby intestinal lesions may have predisposed the calf to a disseminated thrombogenic syndrome. [11]

From the Animal Disease Diagnostic Laboratory, Purdue University, West Lafayette, IN 47907.

Received for publication August 10, 1992.

We report the necropsy and ancillary findings of a female Charolais calf that died following massive ischemic necrosis of hind limb musculature caused by an occluding aortic-iliac thromboembolus. The source of the thromboembolus was an intracardiac thrombus attached to a vegetative lesion of the left atrioventricular valve. To our knowledge, aortic-iliac thromboembolism secondary to valvular endocarditis has not been previously reported in cattle.

A pastured, 650 lb, 6-month-old female Charolais calf with no prior history of clinical illness was observed separated from the main herd. Within a few hours, the calf was found recumbent with posterior paresis, cold hind limbs, pyrexia (rectal temperature of 106 F), hyperpnea, and tachycardia. The calf died 24 hours following observed onset of clinical signs.

At necropsy the septal leaflet of the left atrioventricular valve was effaced by a granular, mottled, light tan-red, ovoid 2 x 4-cm mass (Fig. 1). Extending from this mass into the proximal 8 cm of the aorta was a dark red thrombus. A 1 -cm circular portion of the adjacent anterior left ventricular free wall was depressed and eroded (Fig. 1). In the subendocardial myocardium of both the left and right ventricle, there were multiple 0.2-1.0-cm circular white foci.

The lumina of the distal abdominal aorta and proximal right and left iliac arteries were occluded by a laminated, light tan saddle thromboembolus (Fig. 2). The saddle thromboembolus was easily removed with no attachment to vessel